RAA 2018 Vol. **18** No. **4**, 46(10pp) doi: 10.1088/1674–4527/18/4/46

http://www.raa-journal.org *http://iopscience.iop.org/raa*

Research in Astronomy and Astrophysics

Observations and light curve solutions of a selection of middle-contact W UMa binaries

Diana Petrova Kjurkchieva[1], Velimir Angelov Popov[1,2], Doroteya Lyubenova Vasileva[1] and Nikola Ivanov Petrov[3]

[1] Department of Physics, Shumen University, 115 Universitetska Str., 9712 Shumen, Bulgaria; *d.kyurkchieva@shu.bg*

[2] IRIDA Observatory, Rozhen NAO, Bulgaria

[3] Institute of Astronomy and NAO, Bulgarian Academy of Sciences, 72 Tsarigradsko Shose Blvd., 1784 Sofia, Bulgaria

Received 2017 September 20; Accepted 2018 January 17

Abstract Photometric observations in Sloan g' and i' bands of W UMa binaries NSVS 4340949, T-Dra0–00959, GSC 03950–00707, NSVS 4665041, NSVS 4803568, MM Peg, MM Com and NSVS 4751449 are presented. The light curve solutions revealed that the components of each target are of G and K spectral types. The binaries of the sample have middle-contact configurations whose fillout factors are within the range 0.2–0.4. The only exception is NSVS 4751449 which is in deeper contact (fillout factor of 0.55). It precisely obeys the relation between mass ratio and fillout factor for deep, low mass ratio overcontact binaries. One of the eclipses of almost all targets (except MM Peg) is an occultation and their photometric mass ratios and solutions could be accepted with confidence. We found that the target components have almost equal temperatures but differ considerably in size and mass. The components of the partially-eclipsed MM Peg have close parameters. Our solutions reveal that NSVS 4340949, T-Dra0–00959, NSVS 4803568 and MM Com are of W subtype while GSC 03950–00707, NSVS 4665041, MM Peg and NSVS 4751449 are of A subtype. This subclassification is well-determined for all totally-eclipsed binaries. The targets confirm the trends in which W-subtype systems have smaller periods and lower temperatures than A subtype binaries.

Key words: binaries: close — binaries: eclipsing — stars: fundamental parameters — stars: late-type

1 INTRODUCTION

W UMa type stars are binaries of spectral type F0-K5 whose components share a common envelope (CE) lying between the inner and outer Lagrangian equipotential surfaces and have nearly equal surface temperatures. It is supposed that W UMa systems result from the evolution of wide binaries by angular momentum loss (AML) and mass-ratio reversals (Qian 2003; Stepien 2006). When their primaries ascend the giant branch, mass transfer via Roche-lobe overflow marks the beginning of a CE phase (Willems & Kolb 2004). At this stage the two stars orbit within a single envelope of material, quickly losing angular momentum and spiraling towards each other (Webbink 1984; Ivanova et al. 2013).

Common-envelope evolution (CEE) is a short-lived phase in the life of a large number and wide diversity of binary stars that are progenitors of Type Ia supernovae, X-ray binaries and double neutron stars (Ivanova et al. 2013). V1309 Sco was the first case of direct observational evidence showing that contact binary systems indeed end their evolution by merging into single objects. Hence, the most important role for W UMa stars in modern astrophysics is that they give information on the processes of tidal interaction, mass loss and mass transfer, AML, and merging or fusion of the stars (Martin et al.

2011). However, the questions of when CEE leads to envelope ejection (and a tighter binary) and when to a merger are currently unanswered.

Binnendijk (1970) introduced subdivision of contact binary stars into A and W subtypes based on a main criterion: for A-type the hotter component is the larger star; for W-type the hotter component is the smaller star. The latter binaries are recognized by the primary minima which are occultations (indicating that the small components are the hotter ones). Additional criteria for W/A subclassification were subsequently found: (i) the A type systems are earlier than the W type binaries and the borderline is at 6000–6200 K (Ruciński 1973, Rucinski 1974); (ii) W-type binaries have shorter periods (Smith 1984); (iii) the mass ratios of A type are smaller than those of W type (Ruciński 1973; Smith 1984).

The W/A subclassification poses the problem about the evolutional connection between the two types of W UMa binaries as well as about the W-type phenomenon itself. But sometimes (at least for partial eclipses), the photometric solutions of W UMa light curves appear to be ambiguous since both A and W configurations can fit the observations well (van Hamme 1982; Lapasset & Claria 1986). Then only a simultaneous light curve and radial velocity curve solution can provide a decisive choice between the two alternatives. However, the mass ratio of W UMa binaries is very seldom available from spectral data due to their faintness. Moreover, the rapid rotation of their components does not allow obtaining a precise spectral mass ratio from measurement of their highly broadened and blended spectral lines (Bilir et al. 2005; Dall & Schmidtobreick 2005).

The models of W UMa systems (Li et al. 2004; Li et al. 2005) had shown that W UMa systems evolve into contact binaries with extreme mass ratios and then evolve into single, fast-rotating stars (FK Com stars) or blue stragglers due to Darwin instability when the spin angular momentum of the system is more than a third of its orbital angular momentum (Hut 1980; Eggleton & Kiseleva-Eggleton 2001).

The creation of a binary evolutional scheme requires knowledge of the fundamental parameters of components in W UMa binaries. The main goal of our intensive study of such targets (Kjurkchieva & Vasileva 2015; Kjurkchieva et al. 2015b; Kjurkchieva et al. 2015a; Kjurkchieva et al. 2016b; Kjurkchieva et al. 2016a; Kjurkchieva et al. 2016c; Kjurkchieva et al. 2017a; Kjurkchieva et al. 2017b) is to determine their parameters by light curve solutions of our own data. They can be used also for improving the empirical relations describing W UMa-type systems.

In this paper we present photometric observations and light curve solutions of eight W UMa binaries: NSVS 4340949, T-Dra0–00959, GSC 03950–00707, NSVS 4665041, NSVS 4803568, MM Peg, MM Com and NSVS 4751449. Table 1 presents the coordinates of these targets and available information on their light variability.

2 OBSERVATIONS

The CCD photometric observations of the targets in Sloan g', i' bands were carried out at Rozhen Observatory with the 30-cm Ritchey Chretien Astrograph (located in the *IRIDA South* dome) using an ATIK 4000M CCD camera (2048×2048 pixels, 7.4 μm pixel^{-1}, field of view 35×35 arcmin). Information on our observations is presented in Table 2. GSC 03950–00707 was observed also in $BVIc$ filters (Table 3).

Twilight flat fields were obtained for each filter, and dark and bias frames were also taken throughout the run. The standard procedure was used for reduction of the photometric data (de-biasing, dark frame subtraction and flat-fielding) by software AIP4WIN2.0 (Berry & Burnell 2005).

We performed ensemble aperture photometry with the software VPHOT. The use of numerous comparison stars considerably increases the statistical accuracy of the comparison magnitude (Gilliland & Brown 1988; Honeycutt 1992). Tables 4–5 present the coordinates of the comparison and check stars from the UCAC4 catalog (Zacharias et al. 2013) and their magnitudes from the APASS DR9 catalog (Henden 2016).

3 LIGHT CURVE SOLUTIONS

The IRIDA light curves of the targets were solved using the code PHOEBE (Prša & Zwitter 2005). It is based on the Wilson–Devinney (WD) code (Wilson & Devinney 1971; Wilson 1979; Wilson 1993) but also provides a graphical user interface along with other improvements, including updated filters like Sloan ones used in our observations.

Mean temperatures T_m of the binaries were determined in advance on the basis of their infrared color in-

Table 1 Parameters of Our Targets from the VSX Database

Target	RA	Dec	Period [d]	mag	Ampl [mag]	Type
NSVS 4340949	04 41 01.05	+38 56 10.6	0.304162	14.77 ($R1$)	1.75	EW
T-Dra0–00959	16 27 44.16	+56 45 59.3	0.3293313	11.410 (R)	0.58	EC
GSC 03950–00707	20 35 50.83	+52 42 13.6	0.412	13.28 (V)	0.42	EW
NSVS 4665041	07 16 38.88	+50 00 56.9	0.370556	11.159 ($R1$)	0.52	EB/EW
NSVS 4803568	08 15 16.14	+40 53 31.7	0.28657414	11.674 ($R1$)	0.49	EW
MM Peg	22 21 11.0	+28 03 26.8	0.42609	15.03 (V)	0.30	EW
MM Com	13 00 11.70	+30 23 10.5	0.3019899	12.25 (clear)	0.64	EW
NSVS 4751449	07 45 39.36	+50 12 25.9	0.352648	12.219 ($R1$)	0.49	EB/EW

Table 2 Log of Our Photometric Observations

Target	Date	Exposure (g', i') [s]	Number (g', i')	Error (g', i') [mag]
NSVS 4340949	2016 Nov 18	90, 120	95, 95	0.007, 0.008
	2016 Nov 19	90, 120	106, 106	0.008, 0.009
	2016 Nov 20	90, 120	61, 61	0.006, 0.007
T-Dra0–00959	2016 Jul 11	60, 120	86, 86	0.003, 0.004
	2016 Jul 12	60, 120	27, 25	0.003, 0.004
	2016 Jul 13	60, 120	53, 51	0.003, 0.003
	2016 Jul 14	60, 120	88, 87	0.003, 0.004
	2016 Jul 16	60, 120	43, 42	0.004, 0.003
	2016 Jul 21	60, 120	104, 105	0.003, 0.004
NSVS 4665041	2016 Dec 11	40, 90	162, 162	0.003, 0.004
	2016 Dec 17	40, 90	126, 126	0.003, 0.004
	2016 Dec 18	40, 90	191, 191	0.002, 0.003
NSVS 4803568	2015 Feb 21	60, 90	148, 147	0.003, 0.004
	2015 Mar 3	60, 90	31, 30	0.003, 0.004
MM Peg	2016 Sep 22	120, -	58, -	0.018, -
	2016 Sep 23	120, -	79, -	0.0114, -
	2016 Sep 24	120, -	90, -	0.014, -
	2016 Sep 27	240, -	59, -	0.011, -
	2016 Sep 29	240, -	108, -	0.007, -
	2016 Sep 30	-, 300	-, 87	-, 0.014
	2016 Oct 1	-, 300	-, 88	-, 0.014
MM Com	2015 Jun 1	90, 120	66, 66	0.005, 0.005
	2015 Jun 12	90, 120	42, 42	0.004, 0.005
	2015 Jun 13	90, 120	55, 55	0.003, 0.005
NSVS 4751449	2017 Jan 22	90, 120	94, 94	0.004, 0.006
	2017 Jan 23	90, 120	105, 105	0.004, 0.006

dices $(J - K)$ from the 2MASS catalog and the compilation of color-temperature from Cox (2000).

The initial runs revealed that all targets are overcontact systems. Hence, we applied mode "Overcontact binary not in thermal contact" in the code. The fit quality was estimated by the χ^2 value. The formal convention of the deeper minimum being the primary eclipse (phase 0.0) was accepted.

An additional qualitative consideration before the fitting procedure was the eclipse shape. We noted that the light curves of seven of our targets (MM Peg is the only exception) reveal eclipses with flat bottoms (Figs. 1–2), i.e. occultations. If this is the primary minimum, the target should be of W subtype while the flat secondary eclipse means an A subtype W UMa star. For partially-eclipsed MM Peg with equally-deep eclipses, the only preliminary consideration was to search for a solution corresponding to components with close parameters.

Firstly we fixed $T_1 = T_m$ and varied the initial epoch T_0 and period P to search for fitting the phases of light minima and maxima. After that, we fixed their values and varied simultaneously secondary temperature T_2, orbital inclination i, mass ratio q and potential Ω to search for fit of the whole light curves. The data in i' and g' bands were modeled simultaneously.

Table 3 Log of Our Photometric Observations for GSC 03950–00707

Date	Exposure (g', i', B, V, Ic) [s]	Number (g', i', B, V, Ic)	Error (g', i', B, V, Ic) [mag]
2015 Aug 29	15, 40, -, -, -	247, 256, -, -, -	0.028, 0.023, -, -, -
2015 Aug 30	15, 40, -, -, -	196, 200, -, -, -	0.026, 0.024, -, -, -
2015 Aug 31	-, -, 40, 15, 40	-, -, 93, 92, 87	-, -, 0.026, 0.020, 0.023
2015 Sep 1	-, -, 40, 15, 40	-, -, 101, 88, 93	-, -, 0.025, 0.019, 0.022
2015 Sep 2	-, -, 40, 15, 40	-, -, 138, 139, 136	-, -, 0.025, 0.020, 0.023

Table 4 List of Standard Stars

Label	Star ID	RA	Dec	g'	i'
Target	NSVS 4340949	04 41 01.05	+38 56 10.6	13.98	12.77
Chk	UCAC4 645–020362	04 40 24.28	+38 57 53.18	13.562	12.307
C1	UCAC4 646–020885	04 41 36.08	+39 00 19.56	15.270	12.948
C2	UCAC4 646–020826	04 41 05.14	+39 01 35.94	13.641	13.027
C3	UCAC4 646–020821	04 41 03.81	+39 02 45.71	14.148	12.724
C4	UCAC4 646–020762	04 40 29.03	+39 02 12.05	13.555	12.497
C5	UCAC4 645–020369	04 40 28.84	+38 58 24.85	14.373	12.206
C6	UCAC4 645–020413	04 40 55.46	+38 57 16.88	14.416	13.401
C7	UCAC4 645–020415	04 40 56.07	+38 56 54.09	15.096	13.233
C8	UCAC4 645–020398	04 40 47.32	+38 56 19.71	14.489	12.307
C9	UCAC4 645–020397	04 40 45.91	+38 54 21.95	15.466	12.690
C10	UCAC4 645–020452	04 41 18.48	+38 51 57.22	14.467	12.353
C11	UCAC4 645–020493	04 41 42.30	+38 57 04.53	14.981	13.447
C12	UCAC4 645–020373	04 40 30.90	+38 55 20.01	14.071	12.940
Target	T-Dra0–00959	16 27 44.16	+56 45 59.3	11.64	11.09
Chk	UCAC4 734–055067	16 27 01.62	+56 41 07.24	13.124	13.309
C1	UCAC4 735–055893	16 27 09.54	+56 53 00.63	12.929	12.400
C2	UCAC4 735–055916	16 28 25.20	+56 48 37.52	12.013	11.416
C3	UCAC4 734–055086	16 27 30.97	+56 44 03.86	12.575	12.069
C4	UCAC4 734–055063	16 26 38.06	+56 41 54.87	12.853	12.521
C5	UCAC4 735–055896	16 27 18.76	+56 48 43.25	13.382	12.461
C6	UCAC4 734–055065	16 26 57.73	+56 37 48.05	13.002	12.413
C7	UCAC4 733–057093	16 28 29.75	+56 33 34.72	12.690	12.211
C8	UCAC4 733–057087	16 28 09.01	+56 33 25.88	12.820	12.400
Target	NSVS 4665041	07 16 38.88	+50 00 56.9	11.20	10.69
Chk	UCAC4 700–047962	07 16 14.67	+49 57 36.01	13.017	12.464
C1	UCAC4 701–047669	07 16 32.75	+50 08 52.70	12.064	11.407
C2	UCAC4 701–047651	07 15 57.51	+50 05 06.84	12.836	12.333
C3	UCAC4 701–047735	07 17 57.25	+50 01 33.97	12.952	12.026
C4	UCAC4 701–047693	07 17 01.46	+50 02 02.32	11.584	11.133
C5	UCAC4 700–048030	07 17 36.06	+49 53 51.60	12.601	12.133
C6	UCAC4 700–047940	07 15 42.84	+49 58 35.65	12.157	11.604
C7	UCAC4 700–047949	07 15 56.23	+49 59 22.18	13.056	12.259
C8	UCAC4 700–047981	07 16 48.25	+49 59 44.06	11.859	10.864
C9	UCAC4 700–047994	07 17 01.21	+49 55 56.56	13.076	12.773
Target	NSVS 4803568	08 15 16.08	+40 53 19.7	12.07	12.26
Chk	UCAC4–655–050328	08 15 12.08	+40 52 46.39	13.571	13.065
C1	UCAC4–655–050327	08 15 09.81	+40 59 40.51	12.427	11.841
C2	UCAC4–656–049873	08 14 37.92	+41 02 05.37	13.077	11.854
C3	UCAC4–656–049872	08 14 32.66	+41 01 18.66	12.759	12.070
C4	UCAC4–655–050313	08 14 35.33	+40 57 53.10	13.395	12.817
C5	UCAC4–655–050322	08 14 51.23	+40 55 44.47	12.598	12.118
C6	UCAC4–655–050334	08 15 18.82	+40 52 53.80	13.508	12.935
C7	UCAC4–655–050312	08 14 34.13	+40 54 24.62	13.793	13.111
C8	UCAC4–655–050355	08 15 50.08	+40 50 07.22	13.653	12.992
C9	UCAC4–655–050351	08 15 48.10	+40 48 04.59	11.823	10.599
C10	UCAC4–654–049282	08 14 39.03	+40 45 16.11	13.498	12.664
Target	MM Peg	22 21 11.05	+28 3 26.23	15.14	14.68
Chk	UCAC4 591–134602	22 21 47.14	+28 05 28.21	14.360	13.201
C1	UCAC4 590–134319	22 21 58.53	+27 57 39.13	13.700	13.190
C2	UCAC4 590–134268	22 21 27.93	+27 58 29.23	14.206	13.301
C3	UCAC4 590–134302	22 21 48.22	+27 59 26.26	13.982	13.359

Table 4 — *Continued.*

Label	Star ID	RA	Dec	g'	i'
C4	UCAC4 591–134550	22 21 15.51	+28 04 13.34	13.539	12.884
C5	UCAC4 591–134590	22 21 38.84	+28 05 26.42	13.229	12.297
C6	UCAC4 591–134573	22 21 31.08	+28 07 20.65	13.213	12.615
C7	UCAC4 591–134594	22 21 41.55	+28 08 12.48	13.318	12.713
C8	UCAC4 591–134609	22 21 51.23	+28 08 03.18	13.773	13.106
C9	UCAC4 591–134625	22 21 59.90	+28 05 28.35	13.329	12.661
C10	UCAC4 590–134318	22 21 57.52	+27 55 26.19	13.479	12.254
Target	MM Com	13 00 11.70	+30 23 10.5	12.54	12.32
Chk	UCAC4–602–049693	13 00 19.71	+30 21 10.97	13.712	13.677
C1	UCAC4–603–050773	13 00 24.37	+30 28 08.05	12.387	12.208
C2	UCAC4–603–050757	12 59 24.58	+30 32 17.27	12.174	11.558
C3	UCAC4–602–049707	13 01 12.91	+30 18 37.40	11.777	11.749
C4	UCAC4–602–049699	13 00 53.60	+30 14 15.98	12.527	12.171
C5	UCAC4–602–049691	13 00 14.74	+30 14 27.02	12.325	11.889
C6	UCAC4–601–050659	12 59 42.34	+30 11 19.94	12.766	12.534
Target	NSVS 4751449	07 45 39.36	+50 12 25.9	12.38	11.88
Chk	UCAC4 701–048803	07 45 28.53	+50 09 06.98	12.631	11.987
C1	UCAC4 702–046993	07 44 51.73	+50 18 51.36	12.428	11.223
C2	UCAC4 702–047012	07 45 30.80	+50 17 55.63	13.679	12.989
C3	UCAC4 702–047005	07 45 19.07	+50 20 00.48	13.728	13.169
C4	UCAC4 702–047018	07 45 44.14	+50 16 39.21	13.504	12.107
C5	UCAC4 702–047030	07 46 04.42	+50 14 46.09	13.750	12.740
C6	UCAC4 701–048854	07 46 35.75	+50 10 47.84	12.618	12.113
C7	UCAC4 701–048847	07 46 28.81	+50 07 23.83	13.236	12.599
C8	UCAC4 701–048825	07 45 54.60	+50 03 56.15	13.547	12.967
C9	UCAC4 701–048804	07 45 29.02	+50 00 27.60	13.539	12.969
C10	UCAC4 701–048830	07 46 11.68	+50 05 22.68	13.785	12.675
C11	UCAC4 701–048822	07 45 50.35	+50 02 48.48	12.247	10.856
C12	UCAC4 701–048834	07 46 15.77	+50 06 53.80	13.244	12.542

Table 5 List of Standard Stars for GSC 03950–00707

Label	Star ID	RA	Dec	g'	i'	B	V	Ic
V	GSC 03950–00707	20 35 50.83	+52 42 13.60	13.79	12.63	13.83	13.12	12.29
Chk	UCAC4 714–073376	20 35 42.00	+52 44 17.22	12.191	11.535	11.895	11.535	11.268
C1	UCAC4 715–073721	20 35 52.36	+52 53 58.66	NA	9.752	11.941	10.453	9.326
C2	UCAC4 715–073609	20 35 26.24	+52 51 47.51	13.115	10.482	13.546	11.698	9.952
C3	UCAC4 715–073446	20 34 38.96	+52 53 46.45	NA	11.239	12.135	11.533	11.046
C4	UCAC4 715–073388	20 34 23.03	+52 50 42.71	11.797	11.361	11.81	11.419	11.11
C5	UCAC4 714–073315	20 35 29.08	+52 46 40.80	NA	10.339	10.568	11.0	9.882
C6	UCAC4 714–073150	20 34 44.94	+52 37 05.22	11.233	10.135	11.306	10.464	9.814
C7	UCAC4 714–073426	20 35 53.85	+52 40 04.62	11.957	11.393	12.196	11.657	11.2
C8	UCAC4 714–073050	20 34 20.73	+52 41 40.41	11.26	9.507	11.31	10.178	9.109
C9	UCAC4 715–073433	20 34 34.97	+52 49 53.23	12.437	11.589	12.677	11.94	11.118
C10	UCAC4 714–073193	20 34 54.21	+52 47 58.23	12.804	11.863	12.724	12.078	11.185
C11	UCAC4 714–073237	20 35 06.20	+52 42 21.34	12.413	11.899	12.535	12.023	11.813

Table 6 Values of the Fitted Parameters

Star	T_0	P	Ω	q	i	T_2^{PH}
NSVS 4340949	2457711.50657 (6)	0.304162	5.75(1)	2.37(1)	84.21(6)	4695(14)
T-Dra0–00959	2457581.36951(2)	0.3293313	7.87(1)	4.08(1)	81.30(1)	5549(9)
GSC 03950–00707	2457264.510583(?)	0.412000	2.23(1)	0.205(2)	78.1(2)	5604(100)
NSVS 4665041	2457741.35498(11)	0.370556	2.464(2)	0.322(1)	86.26(4)	5699(37)
NSVS 4803568	2457075.513(?)	0.286573	8.11(2)	4.20(2)	79.5(2)	5335(14)
MM Peg	2457654.40765(5)	0.426090	3.509(2)	0.896(1)	62.18(6)	6340(32)
MM Com	2457175.4015(?)	0.3019899	8.59(2)	4.66(2)	80.6(3)	5067(17)
NSVS 4751449	2457776.24119(22)	0.352648	2.262(4)	0.248(2)	83.6(2)	5571(64)

Table 7 Calculated Parameters

Star	T_m	T_1	T_2	r_1	r_2	f	L_2/L_1
NSVS 4340949	4800	4875(14)	4770(14)	0.309(3)	0.459(3)	0.0286	2.4554
T-Dra0–00959	5710	5743(10)	5582(9)	0.278(2)	0.509(2)	0.2367	4.0172
GSC 03950–00707	5710	5729(102)	5623(100)	0.526(3)	0.258(3)	0.1183	0.2243
NSVS 4665041	5950	6009(39)	5758(37)	0.496(2)	0.302(2)	0.2515	0.3113
NSVS 4803568	5440	5448(15)	5343(4)	0.268(3)	0.512(3)	0.0869	3.9677
MM Peg	6533	6620(34)	6427(34)	0.402(2)	0.383(2)	0.1411	0.8171
MM Com	5510	5898(20)	5441(17)	0.268(2)	0.528(2)	0.2388	5.6313
NSVS 4751449	5600	5606(63)	5577(64)	0.532(1)	0.298(1)	0.5512	0.3097

Table 8 Parameters of the Surface Spots

Star	λ	α	β	κ
NSVS 4340949	270(1)	9.8(0.5)	85(1)	0.89(0.01)
T-Dra0–00959	330(1)	21.9(0.9)	82(1)	0.90(0.01)
NSVS 4803568	270(1)	9.2(0.4)	81(1)	0.87(0.01)
MM Com	85(1)	24.0(1.0)	80(1)	0.88(0.01)
NSVS 4751449	250(1)	14.8(0.6)	74(1)	0.89(0.01)

We adopted coefficients of gravity brightening $g_1 = g_2$ = 0.32 and reflection effect $A_1 = A_2$ = 0.5 appropriate for late-type stars while the linear limb-darkening coefficients for each component and each color were updated according to the tables of van Hamme (1993). Solar metallicity was assumed for the targets because they consist of late-type stars from the solar vicinity.

In order to reproduce the light curve distortions, we used cool spots on the primary and varied their parameters (longitude λ, latitude β, angular size α and temperature factor κ).

After reaching the best solution, we varied all parameters (T_2, i, q, Ω, T_0 and *P*) together around the values from the last run and obtained the final model.

In order to obtain stellar temperatures T_1 and T_2 around the mean value T_m we used the formulae (Kjurkchieva & Vasileva 2015)

$$T_1 = T_m + \frac{c\Delta T}{c+1}, \qquad (1)$$

$$T_2 = T_1 - \Delta T, \qquad (2)$$

where $c = L_2/L_1$ (luminosity ratio) and $\Delta T = T_m - T_2^{\rm PH}$ were taken from the final PHOEBE fitting.

Although PHOEBE (as WD) works with potentials, it allows the possibility to directly calculate all values (polar, point, side and back) of the relative radius $r_i = R_i/a$ of each component (R_i is linear radius and a is orbital separation). PHOEBE yields as output parameters bolometric magnitudes $M^i_{\rm bol}$ of the two components in conditional units but their difference $M^2_{\rm bol} - M^1_{\rm bol}$ determines the true luminosity ratio $c = L_2/L_1$. The fillout factor can be calculated from the output parameters of PHOEBE by the formula $f = [\Omega - \Omega(L_1)]/[\Omega(L_2) - \Omega(L_1)]$.

Table 6 contains final values of the fitted stellar parameters: initial epoch T_0; period *P*; mass ratio *q*; inclination *i*; potential Ω; secondary temperature $T_2^{\rm PH}$. Due to the formal PHOEBE errors of the fitted parameters being unreasonably small, we estimated them manually based on the following rule (Dimitrov et al. 2017). The error of parameter b corresponds to a deviation Δb from its final value b^f for which the mean residuals increase by 3$\bar{\sigma}$ ($\bar{\sigma}$ is the mean photometric error of the target).

Table 7 lists the calculated parameters: stellar temperatures $T_{1,2}$; stellar radii $r_{1,2}$ (back values); fillout factor f; luminosity ratio L_2/L_1. Their errors are determined from the uncertainties of output parameters used for their calculation. Table 8 lists information for the spot parameters and the steps of their adjustment.

The synthetic light curves corresponding to our solutions are shown in Figures 1 and 2 as continuous lines.

4 ANALYSIS OF THE RESULTS

The main results from the light curve solutions of our data are as follows:

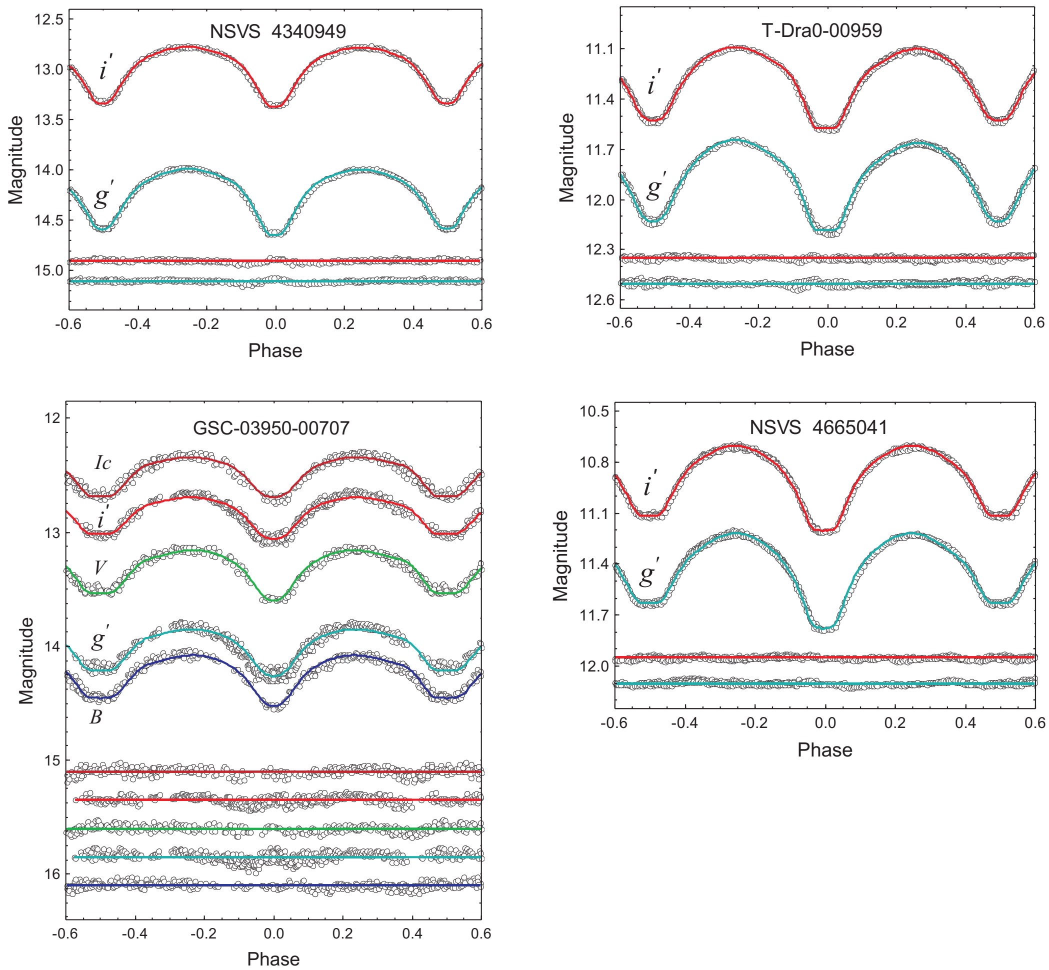

Fig. 1 *Top* of each panel: the folded light curves of the first four targets and their fits; *Bottom*: the corresponding residuals (shifted vertically by different amounts to save space).

(1) We determine the initial epochs T_0 of the all targets (Table 5). It turns out that the previous period values (Table 1) fit our data well.

(2) The amplitude of variability of 1.75 mag for NSVS 4340949 in the VSX database is probably wrong. Our data revealed an amplitude of around 0.5–0.6 mag.

(3) The components of each target are of G and K spectral types (Table 7).

(4) Our observations and light curve solutions reveal that T-Dra0–00959, NSVS 4665041 and NSVS 4751449 are definitely EW type binaries (see Table 1).

(5) All targets have overcontact configurations (Fig. 3, Table 7) with middle fillout factor 0.2–0.4. The only exception is NSVS 4751449 that is in deeper contact. Its fillout factor $f = 0.55$ is close to the dynamical stability limit $f_{\rm ds} = 0.70$ for W UMa systems (Rasio & Shapiro 1995). NSVS 4751449 precisely obeys the relation between q and f for deep, low mass ratio overcontact binaries (eq. (1) in Yang & Qian (2015)). Hence, this target might be close to merging and evolving into a single rapidly-rotating star.

(6) One of the eclipses of almost all targets (except MM Peg) is an occultation. According to Terrell & Wilson (2005) the photometric mass ratios of these overcontact totally-eclipsed binaries should be considered with confidence because the shape of their light curves is sensitive to the mass ratio.

(7) For all targets undergoing occultations, the components are almost the same in temperature but differ considerably in size (by a factor of 1.5–2.0).

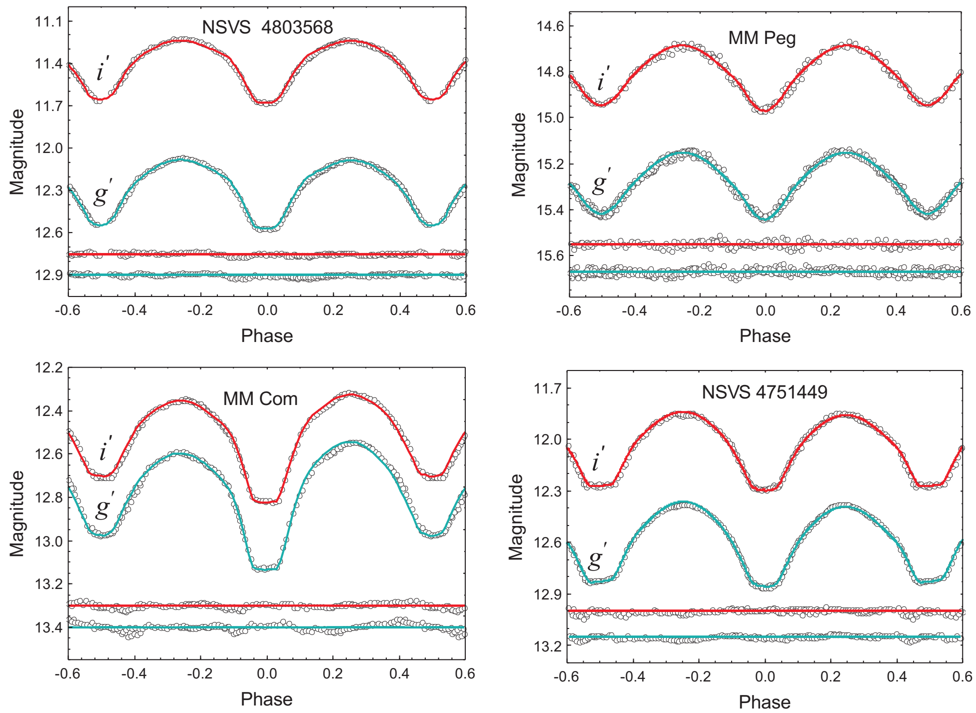

Fig. 2 The same as in Fig. 1 for the last four targets.

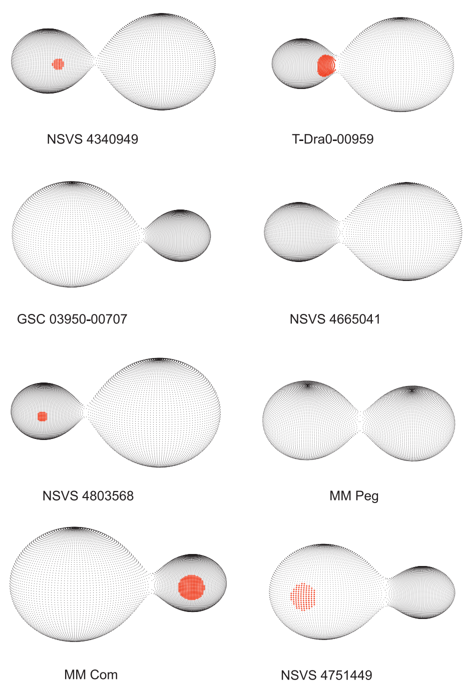

Fig. 3 Three-dimensional configurations of the targets.

(8) The components of the partially-eclipsed MM Peg have close parameters (Tables 6–7).

(9) We found that NSVS 4340949, T-Dra0–00959, NSVS 4803568 and MM Com are of W subtype while GSC 03950–00707, NSVS 4665041, MM Peg and NSVS 4751449 are of A subtype. This subclassification is well-determined for totally-eclipsed binaries (Lapasset & Claria 1986).

(10) We established two trends for our small sample of W UMa stars (Tables 6–7): (i) The subgroup of W-subtype has shorter periods with upper limit of 0.33 d than the targets of A subtype. This is in agreement with the conclusion of Smith (1984) but he gave the mean period value 0.35 d for W subtype; (ii) The subgroup of W-subtype has lower temperatures than the targets of A subtype. This result supports the conclusion of Ruciński (1973) but the borderline between our two subgroups is around 5700 K (lower than the value of 6000–6200 K from Rucinski (1974)).

Our targets with well-determined photometric mass ratios do not confirm the trend of the mass ratios of A subtype being smaller than those of W type (Ruciński 1973, Smith 1984).

(11) The light curve distortions of five binaries are reproduced by cool spots (Table 8) on the side surfaces of their primary components. The spots are manifestations of magnetic activity on these late-type stars.

(12) Although our sample is quite small for a statistical analysis, we note a trend in which the fillout factor f of our targets increases with increases in their primary radius r_1 (or r_2 for $q > 1$ from Tables 6–7).

5 CONCLUSIONS

Our observations and light curve solutions revealed that NSVS 4340949, T-Dra0–00959, GSC 03950–00707, NSVS 4665041, NSVS 4803568, MM Peg, MM Com and NSVS 4751449 are overcontact configurations with middle fillout factors of 0.2–0.4. The only exception is NSVS 4751449 which is in deeper contact (fillout factor of 0.55). It precisely obeys the relation between mass ratio and fillout factor for deep, low mass ratio overcontact binaries.

We found that almost all targets undergo occultations (MM Peg is the only exception). Hence, their photometric mass ratios and solutions could be accepted with confidence. Our results reveal that NSVS 4340949, T-Dra0–00959, NSVS 4803568 and MM Com are of W subtype while GSC 03950–00707, NSVS 4665041, MM Peg and NSVS 4751449 are of A subtype.

This investigation added eight new members to the family of middle-contact W UMa binaries with determined parameters. Our results could be used for improvement of the empirical relations between the parameters of W UMa-type systems, for W/A statistics as well as for elaboration of the binary evolutional scenario.

Acknowledgements This research was supported partly by project DN08/20 of the Scientific Foundation of the Bulgarian Ministry of Education and Science as well as by project RD 02-102 of Shumen University. This publication makes use of data products from the Two Micron All Sky Survey, which is a joint project of the University of Massachusetts and the Infrared Processing and Analysis Center/California Institute of Technology, funded by the National Aeronautics and Space Administration and the National Science Foundation. This research also has made use of the SIMBAD database, operated at CDS, Strasbourg, France, NASA's Astrophysics Data System Abstract Service, the USNOFS Image and Catalogue Archive operated by the United States Naval Observatory, Flagstaff Station (*http://www.nofs.navy.mil/data/fchpix/*) and the photometric software VPHOT operated by the AAVSO, Cambridge, Massachusetts. The authors are very grateful to the anonymous referee for valuable recommendations and notes.

References

Berry, R., & Burnell, J. 2005, The Handbook of Astronomical Image Processing (2nd ed., Richmond, VA: Willmann-Bell)
Bilir, S., Karataş, Y., Demircan, O., & Eker, Z. 2005, MNRAS, 357, 497
Binnendijk, L. 1970, Vistas in Astronomy, 12, 217
Cox, A. N. 2000, Allen's Astrophysical Quantities (4th ed. New York: AIP Press; Springer)
Dall, T. H., & Schmidtobreick, L. 2005, A&A, 429, 625
Dimitrov, D. P., Kjurkchieva, D. P., & Iliev, I. K. 2017, MNRAS, 469, 2089
Eggleton, P. P., & Kiseleva-Eggleton, L. 2001, ApJ, 562, 1012
Gilliland, R. L., & Brown, T. M. 1988, PASP, 100, 754
Henden, A. 2016, Journal of the American Association of Variable Star Observers (JAAVSO), 44, 84
Honeycutt, R. K. 1992, PASP, 104, 435
Hut, P. 1980, A&A, 92, 167
Ivanova, N., Justham, S., Chen, X., et al. 2013, A&A Rev., 21, 59
Kjurkchieva, D. P., Dimitrov, D. P., & Ibryamov, S. I. 2015a, RAA (Research in Astronomy and Astrophysics), 15, 1493
Kjurkchieva, D., Popov, V., Petrov, N., & Ivanov, E. 2015b, Contributions of the Astronomical Observatory Skalnate Pleso, 45, 28

Kjurkchieva, D. P., Popov, V. A., Vasileva, D. L., & Petrov, N. I. 2016a, RAA (Research in Astronomy and Astrophysics), 16, 135
Kjurkchieva, D., Popov, V. A., Vasileva, D., & Petrov, N. 2016b, Serbian Astronomical Journal, 193, 27
Kjurkchieva, D., Popov, V., Vasileva, D., & Petrov, N. 2016c, Serbian Astronomical Journal, 192, 21
Kjurkchieva, D. P., Popov, V. A., Ibryamov, S. I., Vasileva, D. L., & Petrov, N. I. 2017a, RAA (Research in Astronomy and Astrophysics), 17, 042
Kjurkchieva, D. P., Popov, V. A., Vasileva, D. L., & Petrov, N. I. 2017b, RMxAA, 53, 133
Kjurkchieva, D., & Vasileva, D. 2015, PASA, 32, e023
Lapasset, E., & Claria, J. J. 1986, A&A, 161, 264
Li, L., Han, Z., & Zhang, F. 2004, MNRAS, 355, 1383
Li, L., Han, Z., & Zhang, F. 2005, MNRAS, 360, 272
Martin, E. L., Spruit, H. C., & Tata, R. 2011, A&A, 535, A50
Prša, A., & Zwitter, T. 2005, ApJ, 628, 426
Qian, S. 2003, MNRAS, 342, 1260
Rasio, F. A., & Shapiro, S. L. 1995, ApJ, 438, 887
Ruciński, S. M. 1973, Acta Astronomica, 23, 79
Rucinski, S. M. 1974, Acta Astronomica, 24, 119
Smith, R. C. 1984, QJRAS, 25, 405
Stepien, K. 2006, Acta Astronomica, 56, 199
Terrell, D., & Wilson, R. E. 2005, Ap&SS, 296, 221
van Hamme, W. 1982, A&A, 105, 389
van Hamme, W. 1993, AJ, 106, 2096
Webbink, R. F. 1984, ApJ, 277, 355
Willems, B., & Kolb, U. 2004, A&A, 419, 1057
Wilson, R. E. 1979, ApJ, 234, 1054
Wilson, R. E. 1993, in Astronomical Society of the Pacific Conference Series, 38, New Frontiers in Binary Star Research, eds. K.-C. Leung, & I.-S. Nha, 91
Wilson, R. E., & Devinney, E. J. 1971, ApJ, 166, 605
Yang, Y.-G., & Qian, S.-B. 2015, AJ, 150, 69
Zacharias, N., Finch, C. T., Girard, T. M., et al. 2013, AJ, 145, 44